ACS Infectious Diseases

Article

pubs.acs.org/journal/aidcbc

Plantazolicin Is an Ultranarrow-Spectrum Antibiotic That Targets the *Bacillus anthracis* Membrane

Katie J. Molohon,[†,‡,∥] Patricia M. Blair,[#,∥] Seongjin Park,[⊥] James R. Doroghazi,[‡] Tucker Maxson,[#] Jeremy R. Hershfield,[§] Kristen M. Flatt,[Π] Nathan E. Schroeder,[Π] Taekjip Ha,[#,⊥,⊗] and Douglas A. Mitchell*[,†,‡,#]

[†]Department of Microbiology, University of Illinois at Urbana−Champaign, Urbana, Illinois 61801, United States

[‡]Carl R. Woese Institute for Genomic Biology, University of Illinois at Urbana−Champaign, Urbana, Illinois 61801, United States

[#]Department of Chemistry, University of Illinois at Urbana−Champaign, Urbana, Illinois 61801, United States

[⊥]Department of Physics and Center for the Physics of Living Cells, University of Illinois at Urbana−Champaign, Urbana, Illinois 61801, United States

[§]Bacteriology Division, U.S. Army Medical Research Institute of Infectious Diseases, Fort Detrick, Maryland 21702, United States

[Π]Department of Crop Sciences, University of Illinois at Urbana−Champaign, Urbana, Illinois 61801, United States

[⊗]Howard Hughes Medical Institute, Chevy Chase, Maryland 20815, United States

Supporting Information

ABSTRACT: Plantazolicin (PZN) is a ribosomally synthesized and post-translationally modified natural product from *Bacillus methylotrophicus* FZB42 and *Bacillus pumilus*. Extensive tailoring to 12 of the 14 amino acid residues in the mature natural product endows PZN with not only a rigid, polyheterocyclic structure, but also antibacterial activity. Here we report the remarkably discriminatory activity of PZN toward *Bacillus anthracis*, which rivals a previously described gamma (γ) phage lysis assay in distinguishing *B. anthracis* from other members of the *Bacillus cereus* group. We evaluate the underlying cause of this selective activity by measuring the RNA expression profile of PZN-treated *B. anthracis*, which revealed significant up-regulation of genes within the cell envelope stress response. PZN depolarizes the *B. anthracis* membrane like other cell envelope-acting compounds but uniquely localizes to distinct foci within the envelope. Selection and whole-genome sequencing of PZN-resistant mutants of *B. anthracis* implicate a relationship between the action of PZN and cardiolipin (CL) within the membrane. Exogenous CL increases the potency of PZN in wild type *B. anthracis* and promotes the incorporation of fluorescently tagged PZN in the cell envelope. We propose that PZN localizes to and exacerbates structurally compromised regions of the bacterial membrane, which ultimately results in cell lysis.

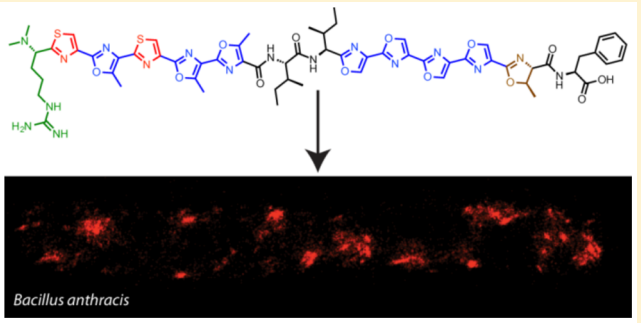

KEYWORDS: *ribosomally synthesized and post-translationally modified natural product, antibiotic, mode of action, pathogen specific antibiotic, membrane depolarization, Bacillus anthracis, anthrax, thiazole, oxazole*

The current practice of employing broad-spectrum antibiotics to treat bacterial infections contributes to the rise of antibiotic resistance.[1] As a countermeasure, species-selective and narrow-spectrum antibacterial compounds are garnering increased attention in the medical community for their potential as therapeutics and/or diagnostics.[2,3] Plantazolicin (PZN) is a polyheterocyclic, linear compound of the ribosomally synthesized and post-translationally modified peptide (RiPP) natural product family with narrow-spectrum antibiotic activity (Figure S1).[4] More specifically, PZN is a member of the thiazole/oxazole-modified microcins (TOMMs), a recently grouped and rapidly expanding RiPP class with ∼1500 identified gene clusters.[5,6] Previously, PZN was described as an antibiotic compound that inhibits Gram-positive organisms closely related to its producing organism, *Bacillus amyloliquefaciens* FZB42[4] (this organism has recently been taxonomically reclassified as *Bacillus methylotrophicus* FZB42).[7] In 2011, by screening a small panel of microorganisms, we described PZN as having potent activity toward *Bacillus anthracis*, but not other Gram-positive pathogens.[8] Several additional PZN-like gene clusters have been identified in six distinct bacterial genera (from three phyla) through genome mining, but experimental data on antibiotic specificity has so far been limited to PZN.[4,8] Although PZN has been the subject of total synthesis,[9−11] heterologous expression,[12] and

Received: October 2, 2015
Published: December 23, 2015

DOI: 10.1021/acsinfecdis.5b00115
ACS Infect. Dis. 2016, 2, 207−220

enzymological studies,[13−15] insight into the mode of action (MOA) of PZN has not been reported in the eight years since the discovery of its biosynthetic gene cluster.[16]

B. anthracis, the causative agent of anthrax and a category A priority pathogen, is a Gram-positive bacterium and a member of the *B. cereus sensu lato* group, which includes *B. cereus*, *B. anthracis*, *B. thuringiensis*, and *B. mycoides*.[17] Microbiologists have debated whether these organisms should be considered as one species, given that some strains share >99% DNA sequence identity. Despite being grouped with other *Bacillus* species, *B. anthracis* harbors a number of distinguishing features compared to other members of the *B. cereus* group. Fully virulent *B. anthracis* contains two conserved plasmids, pXO1 and pXO2, which harbor the genes responsible for producing the anthrax toxin and poly-D-glutamic acid capsule, respectively. However, homologous plasmids are also found in certain *B. cereus* strains.[18] Beyond characteristic plasmid content, *B. anthracis*, unlike other members of the *B. cereus* group, harbors a nonsense mutation in *plcR* (phospholipase C regulator), rendering *B. anthracis* nonmotile and nonhemolytic.[18] The unambiguous differentiation of *B. anthracis* from other nonpathogenic *B. cereus* species is critically important from a public health perspective, especially as it pertains to bioterrorism.

Other defining features of *B. anthracis* that may facilitate species selectivity are exterior to the cell wall. *B. anthracis* displays a two-dimensional protein lattice called the surface layer (S-layer). Decorated with surface-associated proteins in a *csaB* (cell surface attachment)-dependent manner,[19] the S-layer is noncovalently attached to the secondary cell wall polysaccharide (SCWP),[20] which is covalently tethered to the peptidoglycan. The *B. anthracis* SCWP is structurally unique[21] and serves as the binding site for gamma (γ) phage[22,23] and previously described *B. anthracis* typing antibodies.[24] γ phage produce a peptidoglycan hydrolase, PlyG, which specifically recognizes the terminal galactoses of the *B. anthracis* SCWP, allowing efficient digestion of the cell wall.[22] Similarly, typing methods using monoclonal antibodies to the SCWP also exploit differences in the terminal sugar unit. However, there exist atypical *B. anthracis* strains that would constitute false negatives in any diagnostic assay based on these methods.[24,25] Wip1, another *B. anthracis*-specific phage, is even more selective than γ phage, yet certain *B. cereus* strains remain sensitive.[26] Thus, the species specificity of PZN is intriguing not only from a MOA standpoint but also as a rapid means to discriminate *B. anthracis* from other *B. cereus sensu lato* members.

Here we describe PZN as a remarkably selective small molecule antibiotic toward *B. anthracis*. The specificity of PZN was first examined by gene expression profiling, which yielded an expression signature distinct from broader spectrum antibiotics. We have identified and characterized a set of resistant mutants and evaluated their role in PZN resistance, which led us to further investigate the bacterial membrane as the most probable target of PZN. Using fluorescence-based approaches, we confirmed that PZN localizes to the cell envelope in a species-selective manner. PZN binding was associated with rapid and potent membrane depolarization. Taken together with the observation that PZN interacts synergistically with the negatively charged phospholipid, cardiolipin (CL), we propose that PZN localizes to and aggravates transient weaknesses present in the *B. anthracis* cell membrane.

RESULTS AND DISCUSSION

B. anthracis, the causative agent of anthrax, can often be mistaken for other members of the *B. cereus* group. As a bacterium with a history of use in bioterrorism, there is an urgent homeland security need for highly accurate and rapid identification of *B. anthracis*. We therefore set out to characterize and understand the selectivity of PZN.

Defining the Species Selectivity of PZN. PZN was originally described as a Gram-positive antibiotic, inhibiting the growth of *B. subtilis*, *B. cereus*, and *B. megaterium*.[4] It is important to note, however, that the spot-on-lawn assay employed to reach this conclusion used 1 mg of purified PZN per spot. We set out to obtain the minimum inhibitory concentration (MIC) of PZN by using a microbroth dilution assay. As expected, the activity of PZN was revealed to be considerably more selective, in that antibacterial activity was detected toward only *B. anthracis* upon screening of a small panel of human pathogens.[8] We continued to define this unusually narrow spectrum of activity by screening a larger panel of strains with various degrees of genetic similarity (Table S1). PZN was found to be selective for vegetative *B. anthracis*, including fully virulent biosafety level 3 strains, with MICs between 1 and 16 μg/mL (0.75−12 μM). Endospores, the dormant phase of the *B. anthracis* life cycle, were resistant to PZN until germination was initiated (Table S2). By microbroth dilution, *B. subtilis* and *B. cereus* were not susceptible to PZN at concentrations up to 64 μg/mL, which contrasts with the previous spot-on-lawn assay.[4]

To further investigate the selectivity of PZN toward *B. anthracis*, we conducted a head-to-head comparison using the γ phage assay. Prior to modern genomic methods, γ phage sensitivity and other phenotype testing were popular methods for identifying *B. anthracis*.[25] Notwithstanding the reported 96% positive accuracy, non-*B. anthracis* strains that are sensitive to γ phage and true *B. anthracis* strains that are insensitive have been reported.[25,27,28] We obtained a panel of atypical *B. cereus* strains that are sensitive to γ phage and tested them for PZN susceptibility (Table 1). *B. cereus* strains that generated a false positive in the γ phage assay were not susceptible to PZN.[26,28,29]

To further define the attributes giving rise to the species selectivity of PZN, we procured various bacterial strains that address key differences between *B. anthracis* and *B. cereus*. *plcR*, encoding the phospholipase C regulator, is nonfunctional in *B. anthracis* but is intact in *B. cereus*.[18] Deletion of *plcR* in *B. cereus* did not increase its susceptibility to PZN (Table S1). Additionally, sortase-deficient strains of *B. anthracis*, which lack the ability to anchor various proteins to the cell wall, remain susceptible to PZN.[30] The activity of PZN was similarly not dependent on the presence or composition of the *B. anthracis* S-layer, as strains deficient in S-layer assembly or decoration, namely those harboring mutations in *csaB*, *sap*, and *eag*, are equally susceptible to PZN.[19] We further confirmed that susceptibility to PZN is plasmid-independent given that a plasmid-deficient strain (LLNL A0517-1) and strains with both plasmids retained sensitivity (Table S1; Figure S2). Wip1 phage susceptibility and antibody typing have also been used to distinguish *B. cereus sensu lato* strains, but also have known exceptions to their specificity for *B. anthracis*.[24,26] We obtained a "false-positive for *B. anthracis*" strain for each marker: *B. cereus* CDC32805 for Wip1 and *B. cereus* ATCC 7064 for antibody

DOI: 10.1021/acsinfecdis.5b00115
ACS Infect. Dis. 2016, 2, 207−220

Table 1. Susceptibility of *Bacillus* sp. to γ Phage and PZN

strain	γ phage[a]	PZN[b]	source[c]
B. anthracis Sterne 7702	+++	1	USDA
B. anthracis Sterne 34F2 A0517-1[d]	+++	2	BEI
B. cereus 2002013145[e]	+++	>64	CDC
B. cereus 2002013146[e]	+++	>64	CDC
B. cereus 2002013100[e]	++	>64	CDC
B. cereus 2000031002[e]	+++	>64	CDC
B. cereus ATCC 4342	+	>64	ATCC
B. cereus ATCC 7064	+	>64	ATCC
B. cereus CDC 32805	+	>64	26
B. cereus G9241	−	8	BEI
B. megaterium 899	−	32	BGSC
B. mycoides 96/3308	−	>64	BGSC

[a]Plus signs indicate the level of phage sensitivity, with "+++" representing the most sensitive and "−" indicating complete resistance to the phage. [b]Minimum inhibitory concentrations were determined by the microbroth dilution method (μg/mL). [c]Abbreviations: USDA, U.S. Department of Agriculture; BEI, Biodefense and Emerging Infections Research Resources Repository; CDC, U.S. Centers for Disease Control and Prevention; ATCC, American Type Culture Collection; BGSC, Bacillus Genetic Stock Center. [d]LLNL A0517 was obtained from BEI as a mixture of two colony types. A0517_1 was confirmed to be devoid of pXO1 by PCR (Figure S2). [e]Strains identified by multilocus sequence typing analysis.[27]

typing. We again observed no measurable PZN susceptibility for either strain (Table S1).

After extensive susceptibility testing, the only notable exception to the *B. anthracis* selectivity of PZN was *B. cereus* G9241 (MIC of 8 μg/mL). Strain G9241 encodes the genes for an anthrax-like toxin on its pBCXO1 plasmid, which is named for its homology to the *B. anthracis* pXO1 plasmid.[31] Because G9241 is encapsulated and toxigenic, it causes an anthrax-like disease but is undetectable in the γ phage assay.[27] Thus, from a pathogen detection perspective, the action of PZN toward G9241 could be considered fortuitous if it were to be further developed as a rapid diagnostic. Together, these data not only highlight the species discrimination of PZN but also rule out *plcR*-related effects, sortase-mediated proteins, the SCWP, the S-layer, and plasmid-borne entities as targets of PZN.

The spectrum of PZN activity calls into question whether bacteria are the naturally intended target. The canonical PZN-producing strain, *B. methylotrophicus* FZB42 (formerly *amyloliquefaciens*), is a prolific producer of other natural products with antifungal and nematicidal activities.[7,32] Liu et al. ascribed a nematicidal activity to PZN, derived from experiments showing that PZN-deficient FZB42 strains exhibit reduced nematicidal activity against *Caenorhabditis elegans*.[33] Because these experiments employed crude cellular extracts, we evaluated purified PZN in a similar manner, embedding the compound in agar ("slow killing" assay) or providing PZN in a liquid suspension ("liquid fast killing" assay). PZN was found to be no more toxic to *C. elegans* than a vehicle control and is not nematicidal in its own right (Figure S3). Purified PZN was also not responsible for the antifungal activity of the native producer, leaving the ecological function of PZN unknown (Table S1).

After observing the specificity of PZN under one growth medium condition (Luria−Bertani broth, LB), we reassessed specificity against a smaller but representative panel of strains in two additional growth media (Mueller−Hinton and brain−heart infusion broths, Table S3). All tested strains of *B. anthracis* remained equally susceptible, but unexpectedly, some *Staphylococcus aureus* strains were susceptible to PZN under alternative growth media (MICs from 8 to 32 μg/mL). Only *S. aureus* showed media-dependent susceptibility to PZN; all other tested strains remained nonsusceptible to PZN.

Assessing Potential Macromolecules as the Target of PZN. In an attempt to identify the molecular target(s) of PZN by affinity-based purification,[34] three PZN derivatives were prepared: N-terminal biotinylation, C-terminal biotinylation, and C-terminal modification functionalized with aziridinyl and alkynyl groups for photoaffinity capture (Figure S4). Only the C-terminal modifications retained bioactivity, albeit with ∼16-fold reductions; therefore, these probes were utilized for affinity-based target identification. Despite numerous attempts, we were unable to identify interactions unique to PZN compared to the control (data not shown). Because affinity purification-based strategies to identify small molecule targets are most successful when the interaction is of high affinity to a protein,[35] we considered the possibility that PZN may interact with a nonprotein macromolecule. We thus monitored the formation of the cell wall, fatty acids, and RNA (as well as protein) using radiolabeled, biosynthetic precursors in the presence of PZN. Similar to daptomycin and the nisin-like lanthipeptide Pep5, PZN extensively disrupted macromolecular biosynthesis (Figure S5).[36,37] Interestingly, and in contrast to vancomycin and daptomycin, PZN did not significantly block cell wall biosynthesis on the time scale of the experiment.

Gene Expression Signature of PZN. Sublethal antibiotic treatment stimulates rapid transcriptional responses in bacteria, and the induced/repressed genes may be indicative of MOA.[38] We thus performed RNA-Seq to evaluate the transcriptional response of *B. anthracis* following exposure to 0.25 μg/mL (0.25 × MIC) PZN for 10 min.[39] A total of 74 genes were differentially regulated, including 63 up-regulated and 11 down-regulated genes, with an adjusted false discovery rate (*q* value) of 0.01 (Figure 1; Table S4). The expression of a subset of these genes was validated by qRT-PCR (Tables S5 and S6). Fourteen of the up-regulated genes were transporter subunits, a common stress response upon antibiotic treatment.[40] Conversely, PZN treatment led to the down-regulation of genes associated with L-lactate metabolism, for which the implications remain unclear.

The most highly up-regulated *B. anthracis* genes upon PZN treatment were *bas1344* and *bas1345*, which encode a hypothetical protein and a predicted member of the PspA/IM30 family, respectively (Table S6). These genes are homologous to the *B. subtilis* genes *liaI* and *liaH* (lipid II cycle interfering antibiotics), which are involved in the cell envelope stress response. Induction of these genes upon antibiotic treatment is well documented in *B. subtilis*, specifically to antibiotics interacting with lipid II in some capacity (e.g., nisin, vancomycin, and bacitracin).[41] Induction of *liaI* and *liaH* is also seen in *B. subtilis* after daptomycin treatment, despite the lack of any known interaction between daptomycin and lipid II.[42] PZN treatment also results in massive up-regulation of *bas5200* and *bas5201*, which are homologous to a *B. subtilis* thermosensor two-component system (TCS), *desRK*, that regulates the lipid desaturase, *des*.[43] Although *bas5200* and *bas5201* have yet to be experimentally interrogated, the response regulator and adjacent histidine kinase homologues are 62/89% and 38/71% similar/identical at the protein level to *B. subtilis*, respectively. BLAST-P searches using BAS5200 and BAS5201 as the query sequences retrieve

DOI: 10.1021/acsinfecdis.5b00115
ACS Infect. Dis. 2016, 2, 207−220

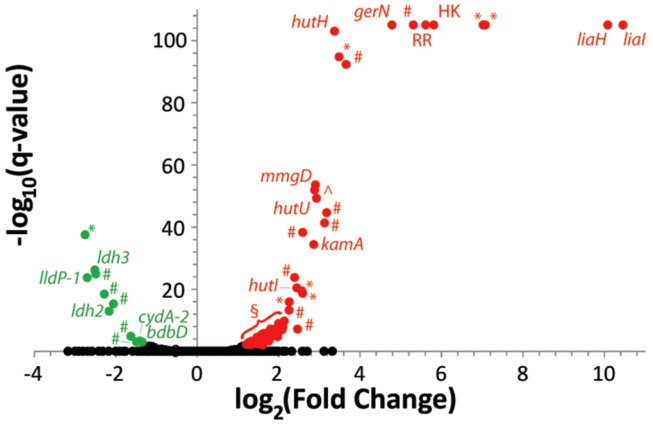

Figure 1. *B. anthracis* gene expression profile when treated with PZN. A volcano plot represents the set of differentially regulated genes in response to a 10 min treatment of PZN at 0.25 × MIC. Red (up-regulated) and green (down-regulated) points are genes with significantly altered expression in response to PZN treatment, whereas black genes did not meet the *q* value (<0.01) threshold. Genes with *q* value = 0 were given an arbitrary value of 1×10^{-105} for graphing purposes. Abbreviations: #, hypothetical; ∗, transporter; ∧, transcriptional regulator; *bdbD*, *B. subtilis* hypothetical homologue; *lldP-1*, L-lactate permease; *ldh2/3*, L-lactate dehydrogenase; *cydA-2*, cytochrome *d* ubiquinol oxidase; *mmgD*, citrate synthase 3; *hutHIU*, histidine utilization genes; *gerN*, germination protein; *kamA*, L-lysine 2,3-aminomutase; §, remaining up-regulated genes. All differentially expressed genes are further described in Table S4.

DesK and DesR as the highest similarity hits in *B. subtilis*; the reverse BLAST-P search (*B. subtilis* DesK and DesR query sequences) likewise retrieves BAS5200 and BAS5201 has the top hits in *B. anthracis*. Pending experimental validation of BAS5200-1 as the bona fide *desRK* TCS in *B. anthracis*, PZN would be to our knowledge the first compound known to alter the expression of these regulators, which is further suggestive of a unique MOA.

Recently, we reported on the synthesis of a PZN derivative, Me_2-Arg-Az_5 (Figure S1).[15] Chemically, Me_2-Arg-Az_5 represents the N-terminal half of PZN, but the activity spectrum of Me_2-Arg-Az_5 is profoundly broader in LB and includes other *Bacillus* species as well as methicillin-resistant *S. aureus* (Table S7). Additionally, the later-described mutations in *bas4114* that conferred resistance to PZN did not confer resistance to other antibiotics or to Me_2-Arg-Az_5 (Tables S7 and S8). To investigate their differing spectra of activity, we recorded the gene expression profile of *B. anthracis* treated with Me_2-Arg-Az_5 under otherwise identical conditions (0.25 × MIC, 10 min) by RNA-Seq. The two compounds shared a minor portion of their expression profiles, but each profile was largely independent (Figure S6; Tables S9 and S10). For example, sublethal Me_2-Arg-Az_5 treatment also induced the *desRK* TCS, but expression of *liaIH* remained unchanged. Additionally, Me_2-Arg-Az_5 failed to induce *B. anthracis* lysis, in contrast to PZN (Figure S7). A possible explanation for the observed differences between PZN and Me_2-Arg-Az_5 is that the C-terminal portion of the molecule is responsible for the species selectivity of the mature molecule and the N-terminal portion harbors the antibiotic activity, although this remains to be more extensively investigated. The expression profiles of PZN and Me_2-Arg-Az_5, together with strain susceptibility, suggest that PZN and Me_2-Arg-Az_5 pursue independent, but possibly related, targets. Thus, although Me_2-Arg-Az_5 is not useful as a mimic for the full-length natural product, it represents one strategy to broaden the antibiotic spectrum of PZN.

PZN Depolarizes the *B. anthracis* Membrane. The induction of *liaIH* and *desRK* by PZN suggests a potential relationship with components of the cell envelope. To

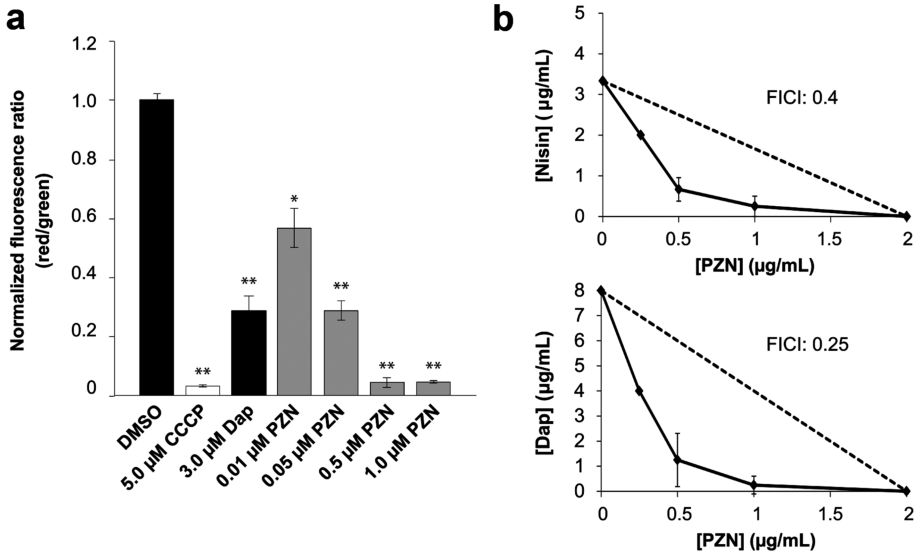

Figure 2. PZN depolarizes the *B. anthracis* membrane and acts synergistically with cell envelope-acting antibiotics. (a) Detection of membrane potential in *B. anthracis*. Red/green ratios were calculated using mean fluorescence intensities of cells treated for 30 min at room temperature with 0.1 μM $DiOC_2(3)$ and the vehicle of DMSO (negative control), 0.1 μM $DiOC_2(3)$ and 5.0 μM CCCP (positive control), 0.1 μM $DiOC_2(3)$ and 0.5 μM PZN, and 0.1 μM $DiOC_2(3)$ and 1.0 μM PZN. Data were normalized to the positive control sample of $DiOC_2(3)$ and vehicle (DMSO). Error is given as standard deviation with $n = 3$. *P* values are given relative to the DMSO control with ∗ indicating <0.0005 and ∗∗ indicating <0.0001. Abbreviations: Dap, daptomycin; $DiOC_2(3)$, 3,3′-diethyloxacarbocyanine iodide; CCCP, carbonyl cyanide *m*-chlorophenyl hydrazone. (b) Isobolograms of the minimum inhibitory concentrations (μg/mL) of PZN with nisin (top) and daptomycin (bottom). Interactions taking place below the dotted line with a fractional inhibitory concentration index below 0.5 represent synergistic behavior.

DOI: 10.1021/acsinfecdis.5b00115
ACS Infect. Dis. 2016, 2, 207−220

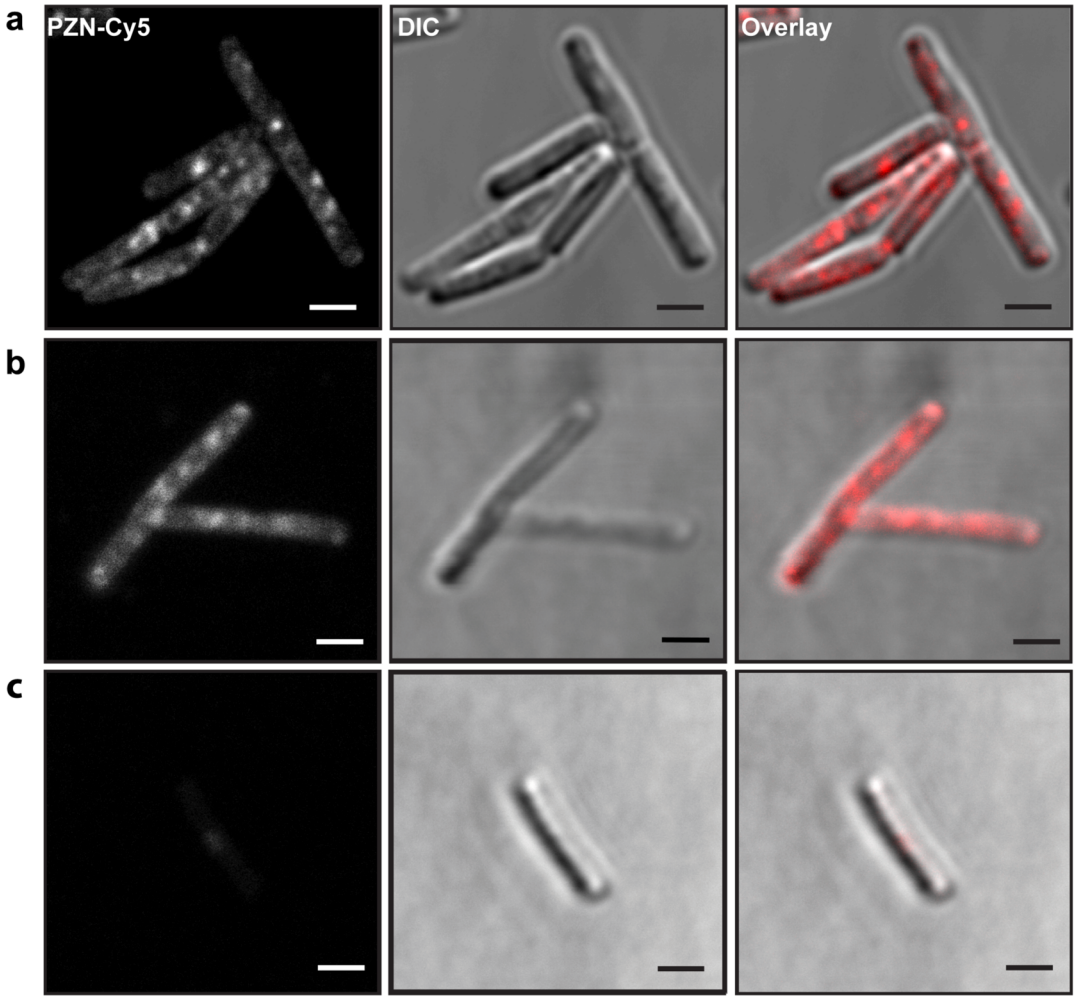

Figure 3. PZN-Cy5 localizes to distinct foci on *B. anthracis*. (a) Representative fluorescence microscopy images are shown for the Cy5, DIC, and merged channels of *B. anthracis* Sterne treated with 0.1 μM PZN-Cy5 (0.05 × MIC) for 30 min. Competition experiments in a PZN-resistant *B. anthracis* strain (PR06, vide infra) show (b) robust labeling with 0.05 μM PZN-Cy5 in the absence of unlabeled PZN and (c) significantly decreased labeling when cells are pretreated with 1 μM PZN (0.016 × MIC, resistant strain PR06) for 20 min. Scale bars = 2 μm.

determine if PZN treatment led to the loss of membrane potential, 3,3′-diethyloxacarbocyanine iodide ($DiOC_2(3)$) was used in a standard flow cytometry-based assay.[44] We observed a dose-dependent decrease in membrane potential upon treating *B. anthracis* with PZN, even at concentrations 100-fold below the MIC. These data further suggest that PZN exerts its action by disrupting the integrity of the cell membrane (Figure 2). Destabilization of the bacterial cell membrane is a common MOA for antibiotics; for example, both nisin and daptomycin are known to disrupt membrane potential in Gram-positive organisms.[45−47] By cotreating *B. anthracis* with either nisin or daptomycin and PZN, the resulting isobolograms elicited strong synergistic activity with PZN (Figure 2), suggesting independent but cooperative activities.[48]

Subcellular Localization of PZN. With mounting evidence that PZN targets the cell membrane, we determined the subcellular localization of PZN by confocal microscopy. Antibiotics derivatized with fluorescent probes have previously been used to shed light on their MOAs.[49,50] Localization of PZN was established by employing a Cy5-labeled PZN derivative (PZN-Cy5) (Figures S1 and S8) that retained much of its anti-*B. anthracis* activity (MIC of 4 μg/mL, 2 μM). PZN-Cy5 localized to distinct ∼200 nm wide foci in *B. anthracis* Sterne (Figure 3a). To establish if PZN-Cy5 behaved in a manner identical to that of unlabeled PZN, we carried out a competition assay using an excess of unlabeled PZN applied to *B. anthracis* Sterne followed by addition of PZN-Cy5. Due to the extensive cell lysis elicited by PZN, we employed a later-described, spontaneous PZN-resistant mutant (PR06) for the competition assay. Just as in *B. anthracis* Sterne, PZN-Cy5 localized to distinct foci in *B. anthracis* PR06, which is consistent with its susceptibility, albeit at higher concentrations of PZN (Figure 3b). Importantly, PZN-Cy5 failed to label strain PR06 when an excess of unlabeled PZN was administered first, demonstrating that PZN and the PZN-Cy5 probe identically interact with *B. anthracis* (Figure 3c). Due to the photoswitching properties of Cy5, we were able to further investigate PZN-Cy5 localization using stochastic optical reconstruction microscopy (STORM, Figure 4).[51] Using this super-resolution imaging technique, *B. anthracis* Sterne cells were again confirmed to accumulate PZN-Cy5 at the foci described above. These foci were clearly concentrated near the cellular surface, providing additional evidence that a component of the cell envelope is the target of PZN (Figure S9; Movies S1 and S2). *B. anthracis* cells contain 16 ± 2 foci per cell, each with a diameter of 181 ± 7 nm, as determined by analysis of 14

DOI: 10.1021/acsinfecdis.5b00115
ACS Infect. Dis. 2016, 2, 207−220

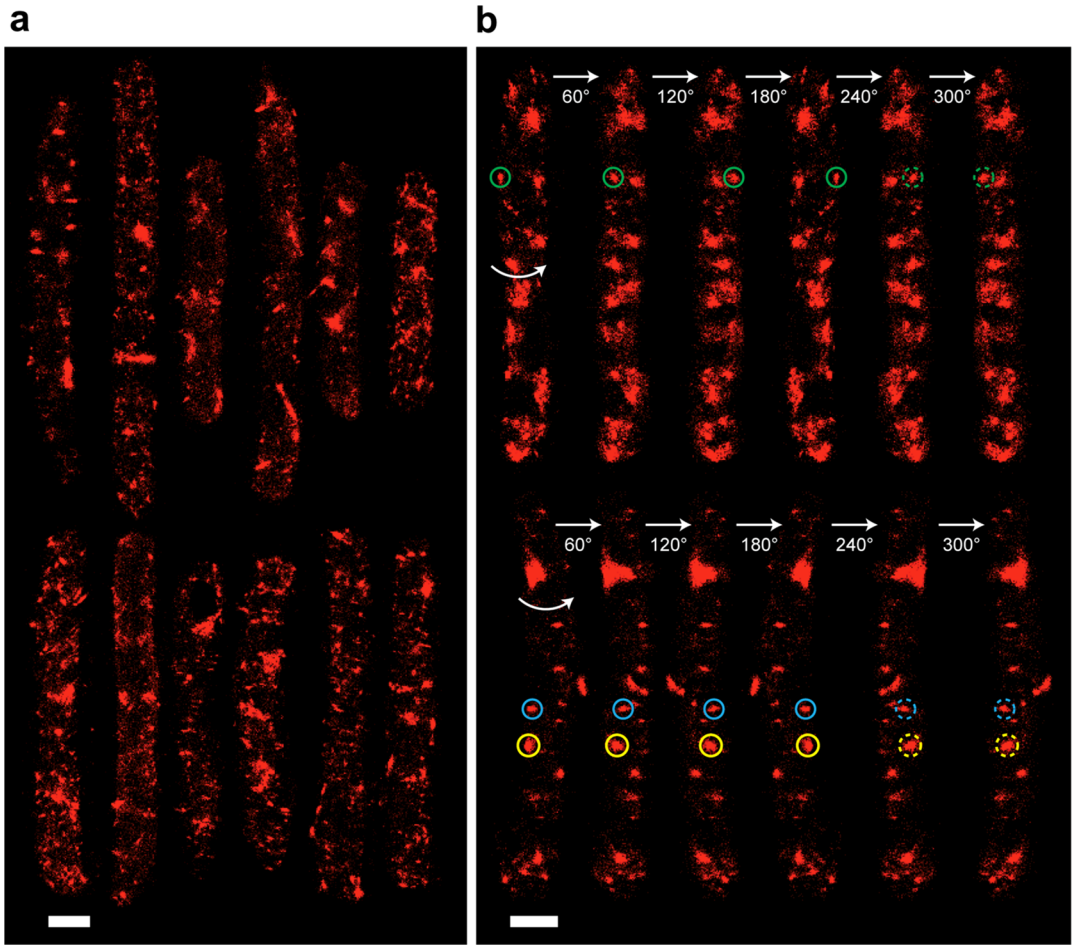

Figure 4. STORM images of PZN-Cy5-labeled *B. anthracis*. (a) 3-D super-resolution images of 12 representative *B. anthracis* cells treated with PZN-Cy5. (b) Two representative cells rotated about the *z*-axis show distinct, nonseptal localization of PZN-Cy5. Green, blue, and yellow circles mark three individual foci in each rotated view. Scale bars = 1 μm.

randomly chosen cells treated with PZN-Cy5 (Figure S9). The labeling pattern of PZN-Cy5 is strikingly different from that of BODIPY-vancomycin, which localizes strongly to bacterial septa where peptidoglycan synthesis is at a maximum.[52] If PZN were acting on the cell wall, sites of active peptidoglycan synthesis or the entire cell wall would be labeled with PZN-Cy5. The nonseptal, punctate labeling of PZN-Cy5 suggests that the target of PZN is neither nascent nor existing peptidoglycan, which is congruent with the observation that PZN did not block cell wall biosynthesis (Figure S5). PZN-Cy5 also does not appear to label nonsusceptible *Bacillus* species (Figure S10). Some modest labeling was found with *B. cereus* G9241, which aligns with a somewhat elevated MIC for PZN (8 μg/mL). Combined with the evidence of PZN-Cy5 labeling PZN-resistant *B. anthracis* PR06 (Figure 3), these data suggest that PZN binding to the cell envelope is necessary, but insufficient, for bacterial killing.

Isolation and Characterization of PZN-Resistant Mutants. An orthogonal strategy for obtaining antibiotic MOA information involves the selection and mapping of resistance-conferring polymorphisms.[53] The mutated gene(s) can be involved either directly in the MOA of the antibiotic or in a target-unrelated mechanism of immunity. We isolated PZN-resistant *B. anthracis* by growing the Sterne strain on agar plates containing PZN at 4 × MIC. The resistance frequency was determined to be 2.3×10^{-7}, and the resulting mutants exhibited MICs that were ≥32 μg/mL. Genomic DNA was isolated and sequenced for six independently selected PZN-resistant strains (PR01 through PR06) and the parent Sterne strain. Comparison of PR01 through PR06 to the parent revealed that all six polymorphisms were confined to a 50-nucleotide section of a single gene, *bas4114*, which is annotated as an AcrR transcriptional repressor (Table S11).[54] This particular AcrR protein is predicted to contain a single transmembrane domain near the C-terminus (Figure S11), which is precisely where the PZN resistance conferring mutations were found, all resulting in premature stop codons. Directly downstream of *bas4114* are two EmrE-type multidrug resistance efflux pumps, encoded as *bas4115−4116*. We hypothesized that as an AcrR-type transcriptional repressor, BAS4114 would negatively regulate *bas4115−4116* and that mutations near the C-terminus of BAS4114 would result in regulator mislocalization/dysfunction and derepression of the efflux pumps. This in turn would increase resistance to PZN. Multidrug resistant transporters have been shown to export membrane-associated antibiotics,[55,56] a concept that is consistent with our data supporting the localization of PZN. One prediction is that BAS4115−6 actively efflux membrane-associated PZN, which lowers the steady-state membrane concentration of PZN. The MIC for PZN thus would increase with the increased expression of *bas4115−4116*. We employed RNA-Seq to compare the mRNA expression profiles of PR06 to

DOI: 10.1021/acsinfecdis.5b00115
ACS Infect. Dis. 2016, 2, 207−220

the parent Sterne strain. This analysis revealed significant up-regulation of *bas4114−4116*, as well as an unknown gene immediately downstream, *bas4117* (Table S12). PR06 and the Sterne parent were equally susceptible to Me_2-Arg-Az_5 (Table S7), again underscoring differences between PZN and Me_2-Arg-Az_5. The susceptibility of PR06 to a panel of mechanistically diverse antibiotics, including daptomycin, was also assessed (Table S8). The mutation present in PR06 did not confer cross-resistance toward any other tested antibiotic. We then investigated if *bas4114−4117* were constitutively overexpressed in nonsusceptible *B. cereus* strains E33L and ATCC 4342, thereby conferring innate resistance to PZN. Using qRT-PCR, we could not identify constitutive overexpression of this locus in nonsusceptible *B. cereus* strains compared to *B. anthracis* (data not shown). This suggests that the *bas4114−4117* locus is not responsible for PZN resistance in nonsusceptible *B. cereus* strains.

Frameshift mutations in the predicted transmembrane region of *bas4114* are clearly the favored route for generating PZN resistance in *B. anthracis*, as shown by the occurrence of multiple independent mutations within the same gene. To subvert this resistance mechanism, and to obtain more insightful information about the MOA of PZN, we deleted *bas4114−4117* from the parental strain by homologous recombination (Figure S12). *B. anthracis* Sterne Δ*bas4114−4117* thus became the new parental strain for isolating second-generation PZN-resistant mutants, as the removal of *bas4114−4117* rendered this strain as sensitive to PZN as wild type Sterne (1 μg/mL). This time, two routes were pursued for obtaining additional PZN-resistant strains. First, we selected spontaneous PZN-resistant mutants by challenging Δ*bas4114−4117* with 4 × MIC PZN. Isolation of the spontaneous mutants resulted in a mutation frequency an order of magnitude lower than before (1.3×10^{-8}). Two independently selected, modestly resistant strains (PR07 and PR08) were subjected to whole-genome sequencing, revealing single missense mutations within *ftsE* (Table 2). In *Escherichia coli*, FtsE is an ATP-binding protein that associates with its cognate permease, FtsX, together comprising an ABC transporter that functions during cell wall elongation and septum formation.[57] The activity of FtsE/X in *B. subtilis* differs slightly, as it is responsible for initiating endospore formation via asymmetric septation.[58] Akin to *bas4114*, spontaneous mutations in *ftsE* alone cannot explain the species selectivity of PZN, as the amino acid sequence of *B. anthracis* FtsE is 100% identical to several nonsusceptible *B. cereus* strains. Other *B. cereus* strains, even the PZN-susceptible G9241 strain, are 98−99% identical to *B. anthracis* FtsE. Although there may be an indirect relationship between PZN and FtsE/X, our data support a MOA that does not involve a physical association with FtsE.

Table 2. PZN-Resistant Mutants of *B. anthracis* Sterne Δ*bas4114−4117*

strain	mutation	annotation	consequence	MIC[a]
PR07	*bas5034*: A425G	cell division ABC transporter, FtsE	E142G	8
PR08	*bas5034*: G270T	cell division ABC transporter, FtsE	L90F	32
PR09-1	*bas1659*: G190C	CitB RR[b]/luxR family	V64L	16
PR09-4	*bas1659*: G190C	CitB RR[b]/luxR family	V64L	>64
	bas1662: A638G	ABC transporter permease	H213R	
PR10-4	*bas1659*: C248T	CitB RR[b]/luxR family	T83M	64
	bas1663: C1127T	ABC transporter permease	A376V	
	bas1842: A43G	petrobactin biosynthesis, AsbE	S15G	

[a]MICs were determined by microbroth dilution assay, measured in μg/mL. [b]Response regulator.

As a second strategy to obtain PZN-resistant mutants, we cultured *B. anthracis* Sterne Δ*bas4114−4117* in the presence of a sublethal concentration of PZN. The concentration of PZN was gradually increased with the number of passages.[59] We isolated genomic DNA from a first-passage strain (PR09-1, MIC 16 μg/mL) in addition to two independent fourth passage strains (PR09-4, PR10-4, MICs ≥ 64 μg/mL) for whole genome sequencing. PR09-1 contained a missense mutation in *bas1659*, which encodes a predicted CitB-like response regulator (Table 2). Downstream of *bas1659* are genes encoding a predicted histidine kinase (*bas1660*), ABC transporter subunits (*bas1661−1663*), and a cardiolipin (CL) synthase gene (*bas1664*). PR09-4 is a descendent of PR09-1, and as such, PR09-4 contained the same *bas1659* mutation as PR09-1 in addition to another missense mutation in *bas1662* (the permease domain of the locally encoded ABC transporter). PR10-4 contained a similar mutation series (*bas1663*, a second permease gene for what is presumably a trimeric ABC transporter) but had an additional mutation in *bas1842*, which is implicated in petrobactin biosynthesis.[60] Upon further inspection, we found that deletion of the petrobactin biosynthetic gene cluster did not decrease susceptibility to PZN; therefore, the significance of this missense mutation remains unknown (Table S1).

Exogenous Cardiolipin Increases Sensitivity to PZN. We hypothesized that the regulatory- and transport-related mutations upstream of the gene encoding CL synthase could alter CL concentrations and, thus, CL may be implicated in the MOA for PZN. We first examined the effect of exogenous CL on the interaction of PZN with the *B. anthracis* cell membrane. *B. anthracis* cells were treated with PZN-Cy5 (1 nM, 0.001 × MIC) in the presence and absence of exogenous CL (up to 100 μg/mL). PZN-Cy5 treated cells were then analyzed by flow cytometry. The extent of PZN-Cy5 binding to *B. anthracis* was significantly increased when cells were cotreated with CL (Figure 5). This result is in contrast to that of daptomycin, which acts on the bacterial membrane but exhibits an antagonistic relationship with CL in Enterococci.[61,62] As predicted, co-administration of CL did not increase the labeling efficiency of daptomycin-Cy5 on *B. anthracis* cells (Figures S1 and S13 and Figure 5).[61] Congruent with these data was the observation that CL potentiated the killing activity of PZN toward *B. anthracis*, but decreased daptomycin susceptibility 4-fold. Indeed, the strongly synergistic behavior with CL enhanced the potency of PZN upward of 16-fold, whereas CL alone had no antibiotic activity at the concentrations tested (Figure 5).

PZN Co-localizes with Cardiolipin and Regions of Increased Fluidity. The genetic and functional association with CL implicates the membrane as the most probable target for PZN. The lipid dye 10-*N*-nonyl acridine orange (NAO) approximates regions of the cell membrane enriched in CL.[63] In *B. subtilis* and *B. cereus*, NAO organizes into distinct foci primarily at the septa and the poles (Figure S14),[64] but it

DOI: 10.1021/acsinfecdis.5b00115
ACS Infect. Dis. 2016, 2, 207−220

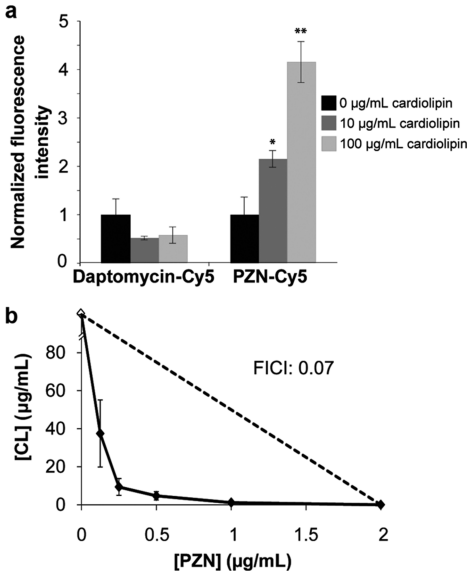

Figure 5. Cardiolipin increases PZN-Cy5 interaction with bacterial cells. (a) Mean fluorescence intensities of *B. anthracis* cell populations treated with daptomycin-Cy5 or PZN-Cy5 in the presence or absence of exogenous cardiolipin (CL) were determined by flow cytometry and normalized to cells treated with only the Cy5-labeled compound and vehicle. Error is reported as standard deviation with $n = 3$. The PZN-Cy5 P values are given relative to the 0 μg/mL control with $*$ indicating <0.01 and $**$ indicating <0.001. The P values for daptomycin-Cy5 were both >0.01. (b) Isobologram of the minimum inhibitory concentrations (μg/mL) of PZN and CL. The Y-intercept was arbitrarily assigned for CL, which in the absence of PZN was not toxic to *B. anthracis* at concentrations up to 200 μg/mL. Interactions taking place below the dotted line with a fractional inhibitory concentration index (FICI) < 0.5 represent synergistic behavior.

appears that in *B. anthracis* Sterne, NAO labels distinct foci throughout the entirety of the cell membrane (Figures 6 and S14). CL has the potential to dramatically alter membrane architecture and may contribute to the susceptibility of *B. anthracis* through punctate localization throughout the cell. We therefore treated *B. anthracis* cells with PZN-Cy5 and NAO to investigate if PZN localized to CL-rich regions in the cell membrane. There existed a clear but imperfect co-localization of the two dyes, suggesting a possible interaction with CL in the bacterial membrane (Figure 6). Thus, *B. anthracis* appears to have a unique distribution of CL that facilitates an interaction with PZN and leads to cell death, whereas CL localization within other species may not facilitate the lytic activity of PZN. Additionally, 1,1′-didodecyl-3,3,3′,3′-tetramethylindocarbocyanine perchlorate, (DilC12(3)), is a dye reported to associate with regions of increased fluidity (RIF) within cell membranes of *B. subtilis* and may also be indicative of CL localization.[65] RIFs are transiently weakened regions within the bacterial membrane that affect lipid homeostasis and membrane fluidity. We observed co-localization of DilC12(3) and PZN-Cy5, consistent with PZN and CL co-associating with *B. anthracis* RIFs (Figure 6).

The proportion of CL in cell membranes has been reported to increase during growth in high-osmolarity medium, especially for *B. subtilis*.[66] We thus tested whether increasing the osmolarity of the *B. subtilis* medium (and thus the CL content) would induce susceptibility to PZN. When grown in standard LB supplemented with an additional 1.5 M NaCl (1.67 M final), PZN was weakly growth-suppressive toward *B. subtilis* (Table 3). By measuring CL from total lipid extractions, CL levels did increase compared to standard growth in LB (Table 3). However, exogenous CL alone did not induce PZN susceptibility in *B. subtilis* or *B. cereus* (data not shown). Members of *B. cereus sensu lato*, including *B. anthracis*, are not as osmotolerant as *B. subtilis*;[67] the maximum salinity these strains can tolerate in LB is 0.67 M (standard LB supplemented with an additional 0.5 M NaCl). When grown under high osmotic stress, both wild type and PZN-resistant strains of *B. anthracis*

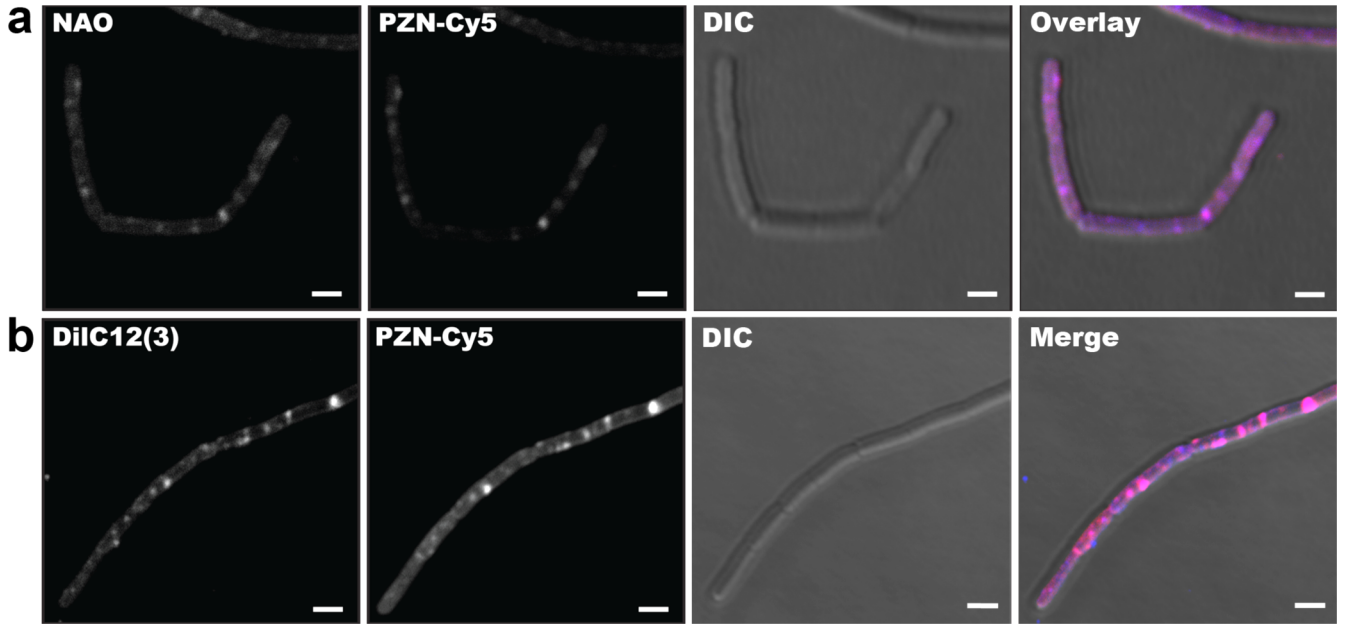

Figure 6. PZN co-localizes with CL- and RIF-specific dyes. (a) From left to right, the channels for NAO, Cy5, DIC, and a merged image are shown to illustrate the false-color co-localization (magenta) of NAO (blue) and PZN (red). (b) The same as panel a but with DilC12(3) replacing NAO. Scale bars = 2 μm.

DOI: 10.1021/acsinfecdis.5b00115
ACS Infect. Dis. 2016, 2, 207−220

Table 3. Effect of *B. anthracis* Sterne Mutations and Growth Conditions on PZN Susceptibility and Cardiolipin Content of Bacterial Membranes

strain	MIC[a]	[NaCl][b]	% CL[c]
B. anthracis Sterne 7702	1	0.17	8.8 ± 4.0
B. anthracis Sterne 7702	0.25	0.67	12.2 ± 3.4
B. anthracis Sterne 7702 Δ*bas4114*–*4117*	1	0.17	11.5 ± 1.3
B. anthracis PR09-4	>64	0.17	14.3 ± 1.7
B. anthracis PR09-4	32	0.67	16.3 ± 0.9
B. anthracis PR10-4	64	0.17	10.7 ± 2.3
B. anthracis PR10-4	16	0.67	11.0 ± 4.3
B. subtilis 168	>128	0.17	16.7 ± 0.7
B. subtilis 168	32	1.67	24.1 ± 0.9*
B. cereus E33L	>64	0.17	11.2 ± 2.0
B. cereus E33L	>64	0.67	18.7 ± 2.0*
B. cereus ATCC 4342	>64	0.17	20.6 ± 5.1
B. cereus ATCC 4342	>64	0.67	21.6 ± 2.6

[a]Minimum inhibitory concentrations (MIC) for PZN were determined by the microbroth dilution method and are reported as μg/mL. [b]The NaCl concentration of the media is given in M (0.17 M is the standard for LB). [c]The percentage of cardiolipin (CL) within the total lipid fraction was determined by a TLC-based densitometric assay. Error is given as standard deviation with $n = 3$. Asterisks indicate $P < 0.05$ relative to the same strain grown in LB with 0.17 M NaCl. PZN was absent from CL quantification experiments.

display measurable susceptibility to PZN, although *B. cereus* strains remain resistant (Table 3). Unlike *B. subtilis*, CL content does not increase significantly when *B. anthracis* or *B. cereus* strains are grown in 0.5 M NaCl, suggesting that the observed susceptibilities may be due to the harsh growth conditions rather than CL content.

Cell survival under conditions of increased osmolarity is dependent on membrane fluctuations with an increase in unsaturated fatty acid composition.[66] Increased CL levels are associated with high osmotic stress in *B. subtilis*, *E. coli*, *Lactococcus lactis*, and others.[66] Furthermore, excess CL within the membrane results in increased fluidity and lipid bilayer deformation, as observed when *B. subtilis* is grown in a high-osmolarity medium (Figure S15).[68] By increasing the osmolarity of the growth medium, we can induce a modest increase in the potency of PZN toward *B. anthracis* (Table 3). The resultant increase in CL, together with the activation of the *des* TCS, presumably shifts the lipid profile to a more fluid composition, which negatively affects membrane integrity. This phenotype is readily observed by confocal microscopy (Figure S15).[69] We hypothesize that PZN takes advantage of an already weakened *B. anthracis* membrane to elicit its selective antibacterial activity.

As stated previously, the stepwise-selected PZN-resistant strains accumulated mutations in genes upstream of one of five CL synthase genes (*cls*, *bas1664*). We analyzed the transcriptional response within the *bas1664* locus, including the upstream regulators/transporters, and observed a dramatic increase in the expression of several genes in PR09-1 and PR09-4, including *bas1664* itself and the nearby ABC transporter genes (*bas1661*–*1663*), but not the locally encoded response regulator and histidine kinase genes (*bas1659*–*1660*, Table S13). In stark contrast, there was no differential expression of any tested gene in the PR10-4 strain. Although these results may seem contradictory, PR10-4 did acquire an additional mutation in a gene responsible for the production of the siderophore petrobactin (Table 2).[70] Given that it is well established that *B. subtilis* experiences iron limitation when grown under high osmotic stress,[71,72] it is possible that PR10-4 handles stress induced by PZN or high NaCl concentrations differently from PR09-1 and PR09-4. Furthermore, CL levels do not necessarily correlate to the number of *cls* transcripts (and there are multiple *cls* genes), which is suggestive of other regulatory mechanisms to avoid overproduction of CL.[73] With respect to PR09-1, PR09-4, and PR10-4, there is a complex relationship between CL content and PZN susceptibility. On the basis of our findings, we expect that in addition to CL, other membrane-associated biomolecules may also contribute to the ability of PZN to destabilize *B. anthracis* cell membranes.

Due to advances in genomics, *B. anthracis*, the causative agent of anthrax, can be distinguished from the other members of the *B. cereus sensu lato* group by whole genome sequencing, multilocus sequence typing, the presence of chromosomal lambdoid prophages, and the presence of a characteristic nonsense mutation in *plcR*.[18,29] An alternative approach to *B. anthracis* identification now includes susceptibility to PZN, which is a natural product exhibiting potent and selective bactericidal activity for *B. anthracis* under standard laboratory conditions. Our data demonstrate that the species selectivity of PZN is even more discriminating than that of the reputedly selective γ phage.[25,26,28,29] Additionally, PZN on its own does not contribute to *B. methylotrophicus* FZB42 antifungal or nematicidal activity. *B. anthracis* is nearly identical to other members of the *B. cereus sensu lato* family and, remarkably, strains of *B. anthracis* selected to interrogate key genetic differences retain their respective susceptibility to PZN. Gene expression analysis, together with confocal and super-resolution microscopy, reveals that PZN operates by a different MOA than previously described cell envelope-targeting antibiotics. Thus, we present a model for PZN activity wherein PZN takes advantage of a locally weakened cell membrane, whether due to RIFs, CL-dependent membrane deformation, or some combination thereof. PZN accumulates to such membrane defects, resulting in membrane depolarization and lysis of *B. anthracis* in a species-specific manner. The activity of PZN suggests an immediate homeland security application, where it could be developed into a rapid *B. anthracis* detection test.

METHODS

Strain and Growth Conditions. All strain references are displayed in Table S1. All strains were grown in LB broth unless otherwise described (10 g/L tryptone, 5 g/L yeast extract, 10 g/L (0.17 M) NaCl). Biosafety level 3 strains of *B. anthracis* were grown on Mueller–Hinton agar. *Neisseria* strains were grown in gonococcal medium base supplemented with Kellogg's I and II.[74] *Streptomyces* endospores were isolated on mannitol soybean flour agar (20 g/L mannitol, 20 g/L soybean flour, 1.5% agar) and used to determine PZN susceptibility in ISP2 (4 g/L yeast extract, 10 g/L malt extract, 4 g/L dextrose). Yeast strains were grown in YPD medium (10 g/L yeast extract, 20 g/L peptone, 20 g/L dextrose). *C. elegans* was cultured on nematode growth medium with *E. coli* OP50. Cultures were supplemented with 1.25 mM $CaCl_2$ when assaying daptomycin susceptibility. In cases when increased osmolarity was desired, the LB was supplemented with additional NaCl (final concentration of 1.67 M).

PZN Bioactivity. PZN and Me_2-Arg-Az_5 bioactivities were determined via microbroth dilution assay as described in the Clinical and Laboratory Standards Institute manual.[75] The

DOI: 10.1021/acsinfecdis.5b00115
ACS Infect. Dis. 2016, 2, 207–220

optical density (OD_{600}) of a stationary phase culture was adjusted to 0.01 and added to a microtiter plate containing serially diluted PZN. Wells were visually inspected for turbidity, and the MIC was determined as the lowest compound concentration that incurred no growth after 16 h. MICs were determined in LB unless growth conditions required an alternative medium (see above). The *S. aureus* media-dependent PZN susceptibility was analyzed using LB, brain−heart infusion (BHI, Bacto), and Mueller−Hinton (BBL) broths. When indicated, CL was added to the medium at 100 μg/mL.

A *B. anthracis* growth curve was generated using Tecan Infinite M200 Pro. *B. anthracis* Sterne 7702 cultures were grown in LB to stationary phase at 37 °C. Cultures were diluted to OD_{600} of 0.05 with fresh LB and allowed to recover to an OD_{600} of 0.35. Cultures were aliquoted into 96-well plates containing PZN and incubated at 37 °C with orbital shaking. OD_{600} was measured every 2 min. Values were normalized to an initial OD_{600} of 0.35 and adjusted to a 1 cm path length. Error bars represent standard deviation of two independent experiments.

A growth curve in the presence of Me_2-Arg-Az_5 was generated as described above with the following differences: *B. anthracis* Sterne 7702 and cultures were grown in duplicate to OD_{600} 1.0 and aliquoted into 96-well plates. Wells were treated with 1:1 dilutions of Me_2-Arg-Az_5 at a maximum concentration of 12 μM. The plate was incubated at 37 °C with orbital shaking, and OD_{600} was measured every 2 min. Values were normalized to an initial OD_{600} of 1.0, adjusted to a 1 cm path length, and averaged at each time point.

Gamma (γ) Phage Sensitivity. γ phage are propagated as described previously[25] using *B. anthracis* Sterne 7702 cells on BHI agar plates, with no visible loss in infectivity. Phage infectivity was tested against a panel of *B. cereus* and *B. anthracis* strains using a serial dilution assay. Stationary phase cultures were adjusted to an OD_{600} of 0.1, and 100 μL was plated on BHI plates. Five microliters of phage stock (2.6×10^8 plaque-forming units/mL) was serially diluted (2-fold) and spotted onto the plates and allowed to dry. After incubation at 37 °C for 16 h, plates were removed and visually inspected for plaques.

RNA Isolation and Transcriptional Profiling of PZN-Treated Sterne Cells. For the compound-treated samples, independent 3 mL cultures of *B. anthracis* Sterne 7702 cells were grown to an OD_{600} of 0.4, and 0.25 × MIC of PZN, 0.25 × MIC Me_2-Arg-Az_5,[15] or an equivalent volume of DMSO was added and allowed to incubate for 10 min at 37 °C. Together with resistant mutant PR06, RNA was isolated and prepared as described previously.[4] RNA-Seq libraries were created using the TruSeq Stranded RNA Sample Prep kit (Illumina, San Diego, CA, USA) after rRNA depletion using the RiboZero Bacteria kit (Epicenter, Madison, WI, USA). Sequencing was performed for 1 × 100 cycles on a HiSeq 2000 with version 3 Chemistry. Transcriptomic data were processed with the Rockhopper version 1.30 pipeline[76] using *B. anthracis* Sterne and *B. anthracis* Ames Ancestor plasmid pXO1 (NC_007322.2) as references. Default values (allowed mismatches 0.15, minimum seed length 0.33, minimum expression of UTRs and ncRNAs 0.5) were used, with the exception that reverse complement reads were used for mapping. The RNA-Seq data discussed in this publication have been deposited in NCBI's Gene Expression Omnibus and are accessible through GEO Series accession no. GSE73343 (http://www.ncbi.nlm.nih.gov/geo/query/acc.cgi?acc=GSE73343).

Membrane Depolarization. Three independent stationary phase cultures of *B. anthracis* Sterne 7702 were used to inoculate fresh LB and grown to OD_{600} of 0.5 at 37 °C with shaking. Aliquots (10 μL) were diluted to 1 mL in PBS containing 0.1 μM $DiOC_2(3)$ and compounds (DMSO, vehicle; 5 μM carbonyl cyanide *m*-chlorophenyl hydrazone (CCCP), 3.0 μM daptomycin, 0.5 μM PZN, 1.0 μM PZN). Cells were mixed at 21 °C for 30 min prior to analysis by flow cytometry (BD LSR II Flow Cytometry Analyzer). Voltages for fluorescein isothiocyanate (FITC) and propidium iodide (PI) fluorescence were set so that average counts per cell were between 10^3 and 10^4. Geometric means for fluorescence ratios were normalized to the control $DiOC_2(3)$ samples.

Confocal Microscopy. In general, cells were prepared by inoculating 5 mL of LB with 200 μL of a stationary phase culture. After growing to an OD_{600} of 0.5 at 37 °C with shaking, 1 mL aliquots were centrifuged (3 min, 8000*g*), decanted, and resuspended in sterile PBS. Slides were prepared by mixing 1:1 (v/v) cell suspensions in PBS and liquefied low gelling temperature agarose (Sigma-Aldrich, 2% w/v in water). All microscopy images were obtained using a Zeiss LSM 700 confocal microscope with a 63×/1.4 Oil DIC objective and processed using Zen 2012 software. Laser intensity and gain were kept at a minimum and held constant for all experiments. Linear contrast was equally applied during image processing. To localize PZN, *B. anthracis* Sterne 7702 was treated in PBS with 0.2 μM PZN-Cy5 for 30 min at 22 °C. After washing in PBS (3 × 500 μL), cells were resuspended in a final volume of 250 μL of PBS. Competition experiments were performed using PR06 (PZN-resistant) in PBS treated with DMSO (vehicle) or 1 μM PZN for 20 min at 22 °C before the addition of 0.05 μM PZN-Cy5. After 20 min at 21 °C, the cells were washed in PBS (3 × 500 μL) and resuspended in a final volume of 250 μL of PBS. Sterne underwent cotreatment in PBS with 0.2 μM PZN-Cy5 for 25 min before the addition of other fluorescent compounds. After 5 min of additional treatment, cells were washed in PBS (5 × 500 μL) and resuspended in a final volume of 250 μL of PBS. Concentrations used were as follows: NAO (Sigma-Aldrich), 1 μM; DilC12(3), 1 μM. For CL experiments, cells were treated with EtOH (vehicle), 10 μg/mL CL, or 100 μg/mL CL in addition to 0.2 μM PZN-Cy5 for 30 min. For high-osmolarity samples, cells were grown to stationary phase in standard LB and diluted into high-osmolarity medium (an additional 1.5 M NaCl was added to *B. subtilis* cultures; 0.50 M for *B. anthracis* and *B. cereus*).

Super-resolution Microscopy (STORM). Cells for 3D super-resolution microscopy were grown and treated with PZN-Cy5 as described for confocal microscopy. The cells were immobilized on a Nunc Lab-Tek 8-well chambered coverglass (Sigma-Aldrich) coated with 0.1% (w/v) poly-L-lysine (Sigma-Aldrich). After 10 min of incubation, unattached cells were removed by washing chambers with sterile PBS. Chambers were filled with 500 μL of imaging buffer (10 mM NaCl, 50 mM Tris-HCl (pH 8.5), 10% w/v glucose). Immediately prior to imaging, cysteamine (Sigma-Aldrich, 10 mM final concentration), catalase (EMD Millipore, 909 U/mL), and pyranose oxidase (Sigma-Aldrich, 4.44 U/mL) were added to the imaging buffer. 3D super-resolution microscopy was performed as described previously.[77,78] Briefly, samples were imaged using an Olympus IX-71 inverted microscope outfitted with a 100× NA 1.4 SaPo oil objective. Mechanical shutters (LS6T2,

DOI: 10.1021/acsinfecdis.5b00115
ACS Infect. Dis. 2016, 2, 207−220

Unibliz) were used to alternatively excite the sample with a red laser (DL640-100-AL-O, Crystalaser) and reactivate Cy5 with a violet laser (405 nm, 20 mW, Spectra Physics Excelsor). The lasers were expanded by 7.5×, reflected by a dichoroic mirror (Semrock FF408/504/581/667/762-Di01-25X36), and sent to the sample chamber with a focusing lens that also creates an incidental angle slightly smaller than the total internal reflection angle, reducing the background signal while allowing illumination of several hundred nanometers along the *z*-axis. The emission signal from the sample was passed through an emission filter (Semrock FF01-594/730-25) and two additional notch filters (Semrock NF01-568/647-25X5.0 and NF01-568U-25) and was imaged on an EMCCD camera (DV887ECS-BV, Andor Tech). A cylindrical lens (SCX-50.8-1000.0-UV-SLMF-520-820, CVI Melles Griot, 2 m focal length) in the emission beam path induced astigmatism for 3D detection.[51] ASI CRISP (Applied Scientific Instrumentation) and a piezo-objective (PI P-721.10) were used to compensate for vertical drift during data collection. The horizontal drift was corrected in the post data acquisition step by the analysis software utilizing the correlation function.[79] The data analysis software was provided by Xiaowei Zhuang[77] and modified for 3D imaging.

Selection of Spontaneous PZN-Resistant Mutants. Spontaneous PZN-resistant mutants were generated by plating 2×10^8 *B. anthracis* Sterne 7702 cells grown to stationary phase onto a PZN plate containing 4 × MIC PZN. Surviving colonies were tested for sustained PZN resistance via microbroth dilution as described above. Resistant mutants PR01, PR02, PR05, and PR06 were subjected to genomic DNA isolation as follows: 3 × 10 mL cultures of each strain were grown to stationary phase, harvested, and resuspended in 400 μL of water. Cells were lysed with 50 μL of 10% SDS and 5 μL of 20 mg/mL RNase solution at 22 °C for 5 min. DNA was isolated via 25:24:1 phenol/chloroform/isoamyl alcohol extraction, followed by addition of 24:1 chloroform/isoamyl alcohol. DNA precipitation via cold isopropyl alcohol and a subsequent 70% ethyl alcohol wash resulted in purified genomic DNA.

After genetic deletion of *bas4114*–*4117* (described in the Supporting Information, methods), a second round of spontaneously resistant mutants to PZN was selected and isolated as above. Serial-passage mutants were isolated as previously described,[59] starting with three independent cultures of an OD_{600} of 0.1 *B. anthracis* Sterne 7702 Δ*bas4114*–*4117* in 0.25 μg/mL (0.25 × MIC) PZN LB. Cultures that grew were diluted to an OD_{600} of 0.1 and subjected to increased concentrations of PZN until cultures were resistant to 64 μg/mL. Cultures were serially passaged onto PZN-free medium to confirm mutant stability. Genomic DNA was isolated as described above. All mutants derived from the Δ*bas4114*–*4117* deletion strain were sequenced as described and assembled via CLC Genomics Workbench, and SNP analysis was performed with Mauve version 2.3.1.

Whole Genome Sequencing and Assembly. Genomic libraries for resequencing were prepared using the TruSeq DNaseq Sample Prep Kit (Illumina). Sequencing was performed on a HiSeq 2000 with version 3 Chemistry for 1 × 100 cycles. SNP and DIP discovery was performed with two different methods. Regarding PR02, PR05, and PR06, CLC Genomics Workbench SNP and DIP discovery pipelines were employed using with the publicly available *B. anthracis* str. Sterne genome NC_005945.1 as a reference. PR01 required de novo assembly with IDBA UD version 1.0.9, followed by whole genome alignment and SNP discovery using Mauve version 2.3.1. Resistant mutants PR03 and PR04 were selected separately and underwent Sanger sequencing after PCR amplification of *bas4114* and sequencing with the *Bam*HI-BAS4114-f primer (Table S5). The WGS data discussed in this publication have been deposited in NCBI's GenBank and are accessible via BioProject accession no. PRJNA295544. Within this BioProject are individual accession numbers for each *B. anthracis* strain (taxId: 1392) for which whole genome sequencing was performed: CP012720, PR01; CP012721, PR02; CP012722, PR05; CP012723, PR06; CP012724, PR07; CP012725, PR08; CP012726, PR09−1; CP012727, PR09−4; CP012728, PR10−4; CP012730, Parent1 (for PR01 through PR06); CP012729, Parent2 (for PR07 through PR10-4).

Effect of Cardiolipin on Fluorescence Intensity. Three independent stationary phase cultures of *B. anthracis* Sterne 7702 were used to inoculate fresh LB (200 μL into 5 mL of LB), and the new cultures were grown to OD_{600} of 0.5 at 37 °C with shaking. Samples were prepared by diluting 10 μL aliquots of culture to 1 mL in PBS containing 1 nM PZN-Cy5 and vehicle (EtOH), 10 μg/mL CL (Sigma-Aldrich), or 100 μg/mL CL. After mixing at 22 °C for 30 min, cells were analyzed by flow cytometry as described above for differences in PZN-Cy5 fluorescence intensity. Geometric means were normalized to the control samples.

Cardiolipin Quantification from Total Lipid Extracts. Cultures of *B. anthracis* Sterne 7702, *B. anthracis* Δ*bas4114*–*4117*, *B. anthracis* PR09-4, *B. anthracis* PR10-4, *B. subtilis* 168, *E. faecium* U503, and *S. aureus* USA300 (three independent 10 mL cultures for each strain) were grown for 20 h at 37 °C. LB containing an additional 1.5 M NaCl was inoculated with 200 μL aliquots of stationary phase cultures of *B. subtilis* 168 or 0.5 M NaCl for *B. anthracis* and *B. cereus* (three independent 10 mL cultures for each strain) and grown for 40 h at 37 °C. The cells were harvested by centrifugation (4000*g*, 10 min, 4 °C) and resuspended in 5 mL of 2:1 $CHCl_3$/MeOH and 1.25 mL of PBS and then extracted for 1 h at 22 °C. The supernatant was removed after centrifugation (4000*g*, 10 min, 4 °C), and layers were washed with 1 mL of $CHCl_3$ and 1 mL of PBS. The organic layer was removed and dried by speed vacuum. The crude lipids were redissolved in 200 μL of $CHCl_3$ and transferred to microfuge tubes and then dried again. The lipids were then dissolved in 20 μL of $CHCl_3$, spotted (2 μL) onto Merck Silica Gel 60 F_{254} analytical TLC plates, and separated using 80:20:5 $CHCl_3$/MeOH/AcOH. Pure CL was used as a standard. The plates were imaged using a Bio-Rad ChemiDoc XRS+. ImageJ was used to subtract background and measure spot density to determine percent CL out of total lipid content.

■ ASSOCIATED CONTENT

Supporting Information

The Supporting Information is available free of charge on the ACS Publications website at DOI: 10.1021/acsinfecdis.5b00115.

Additional methods, supplementary tables, supplementary figures (PDF)

Movie 1(AVI)

Movie 2(AVI)

DOI: 10.1021/acsinfecdis.5b00115
ACS Infect. Dis. 2016, 2, 207−220

AUTHOR INFORMATION

Corresponding Author

*(D.A.M.) E-mail: douglasm@illinois.edu. Mail: 1206 West Gregory Drive, Carl R. Woese Institute for Genomic Biology, Room 3105, University of Illinois, Urbana, IL 61801, USA.

Author Contributions

‖K.J.M. and P.M.B. contributed equally to this work. K.J.M., P.M.B., and D.A.M. conceived and designed the experiments. K.J.M., P.M.B., J.R.D., S.P., J.R.H., and K.M.F. performed the experiments. K.J.M., P.M.B., J.R.D., and D.A.M. analyzed the data. T.M., N.E.S., and T.H. contributed reagents/materials/analysis tools. K.J.M., P.M.B., and D.A.M. wrote the paper. All authors reviewed and approved the paper.

Funding

This work was supported by the U.S. National Institutes of Health (1R01 GM097142 to DAM) and the Defense Threat Reduction Agency under USAMRIID (Project 922141). K.J.M., P.M.B., and J.R.D. were supported in part by a James R. Beck Graduate Research Fellowship, an ACS Medicinal Chemistry Predoctoral Fellowship, and the Carle R. Woese Institute for Genomic Biology Fellows program, respectively. The funders had no role in study design, data collection and analysis, decision to publish, or preparation of the manuscript. Opinions, interpretations, conclusions, and recommendations are those of the authors and are not necessarily endorsed by the U.S. Army.

Notes

The authors declare no competing financial interest.

ACKNOWLEDGMENTS

We are grateful to the Pasteur Institute, BEI Resources, O. Schneewind (University of Chicago), C. Turnbough (University of Alabama Birmingham), U.S. Department of Agriculture, The *Caenorhabditis* Genetics Center, The Bacillus Genetic Stock Center, S. Shozhamannan (The Naval Medical Research Center), V. Fischetti (Rockefeller University), C. Marston (Center for Disease Control and Prevention), D. de Mendoza (Universidad Nacional de Rosario), J. Wells (University of California—San Francisco), J. Helmann (Cornell University), M. So (University of Arizona), P. Hergenrother (University of Illinois at Urbana−Champaign), H. Zhao University of Illinois at Urbana−Champaign), P. Hanna (Univeristy of Michigan), and S. Leppla (National Institute of Allergy and Infectious Diseases) for providing strains and plasmids used in this study; Dr. Yao Shao Qin and Dr. Li Zhengqiu (National University of Singapore) for providing 2-(2-azidoethyl)-2-(but-3-ynyl)-1,3-dioxolane; as well as Teresa Abshire, Stephanie Halasohoris, and Lynda Miller (U.S. Army Medical Research Institute for Infectious Diseases, USAMRIID) for providing us with γ phage and their assistance. We also thank C. Deane for critical review of the manuscript.

ABBREVIATIONS

PZN, plantazolicin; RiPP, ribosomally synthesized and post-translationally modified peptide natural product; TOMM, thiazole/oxazole-modified microcin; MOA, mode of action; SCWP, secondary cell wall polysaccharide; CL, cardiolipin; MIC, minimum inhibitory concentration; Des, lipid desaturase; NAO, 10-*N*-nonyl acridine orange; RIF, regions of increased fluidity; DilC12(3), 1,1′-didodecyl-3,3,3′,3′-tetramethylindocarbocyanine perchlorate

REFERENCES

(1) de Man, P., Verhoeven, B. A., Verbrugh, H. A., Vos, M. C., and van den Anker, J. N. (2000) An antibiotic policy to prevent emergence of resistant bacilli. *Lancet 355*, 973−978.

(2) Wilson, D. N., Harms, J. M., Nierhaus, K. H., Schlunzen, F., and Fucini, P. (2005) Species-specific antibiotic-ribosome interactions: implications for drug development. *Biol. Chem. 386*, 1239−1252.

(3) Payne, D. J. (2008) Desperately seeking new antibiotics. *Science 321*, 1644−1645.

(4) Scholz, R., Molohon, K. J., Nachtigall, J., Vater, J., Markley, A. L., Sussmuth, R. D., Mitchell, D. A., and Borriss, R. (2011) Plantazolicin, a novel microcin B17/streptolysin S-like natural product from *Bacillus amyloliquefaciens* FZB42. *J. Bacteriol. 193*, 215−224.

(5) Arnison, P. G., Bibb, M. J., Bierbaum, G., Bowers, A. A., Bugni, T. S., Bulaj, G., Camarero, J. A., Campopiano, D. J., Challis, G. L., Clardy, J., Cotter, P. D., Craik, D. J., Dawson, M., Dittmann, E., Donadio, S., Dorrestein, P. C., Entian, K. D., Fischbach, M. A., Garavelli, J. S., Goransson, U., Gruber, C. W., Haft, D. H., Hemscheidt, T. K., Hertweck, C., Hill, C., Horswill, A. R., Jaspars, M., Kelly, W. L., Klinman, J. P., Kuipers, O. P., Link, A. J., Liu, W., Marahiel, M. A., Mitchell, D. A., Moll, G. N., Moore, B. S., Muller, R., Nair, S. K., Nes, I. F., Norris, G. E., Olivera, B. M., Onaka, H., Patchett, M. L., Piel, J., Reaney, M. J., Rebuffat, S., Ross, R. P., Sahl, H. G., Schmidt, E. W., Selsted, M. E., Severinov, K., Shen, B., Sivonen, K., Smith, L., Stein, T., Sussmuth, R. D., Tagg, J. R., Tang, G. L., Truman, A. W., Vederas, J. C., Walsh, C. T., Walton, J. D., Wenzel, S. C., Willey, J. M., and van der Donk, W. A. (2013) Ribosomally synthesized and post-translationally modified peptide natural products: overview and recommendations for a universal nomenclature. *Nat. Prod. Rep. 30*, 108−160.

(6) Cox, C. L., Doroghazi, J. R., and Mitchell, D. A. (2015) The genomic landscape of ribosomal peptides containing thiazole and oxazole heterocycles. *BMC Genomics 16*, 778.

(7) Dunlap, C. A., Kim, S. J., Kwon, S. W., and Rooney, A. P. (2015) Phylogenomic analysis shows that *Bacillus amyloliquefaciens* subsp. *plantarum* is a later heterotypic synonym of *Bacillus methylotrophicus*. *Int. J. Syst. Evol. Microbiol. 65*, 2104−2109.

(8) Molohon, K. J., Melby, J. O., Lee, J., Evans, B. S., Dunbar, K. L., Bumpus, S. B., Kelleher, N. L., and Mitchell, D. A. (2011) Structure determination and interception of biosynthetic intermediates for the plantazolicin class of highly discriminating antibiotics. *ACS Chem. Biol. 6*, 1307−1313.

(9) Banala, S., Ensle, P., and Sussmuth, R. D. (2013) Total synthesis of the ribosomally synthesized linear azole-containing peptide plantazolicin A from *Bacillus amyloliquefaciens*. *Angew. Chem., Int. Ed. 52*, 9518−9523.

(10) Wilson, Z. E., Fenner, S., and Ley, S. V. (2015) Total syntheses of linear polythiazole/oxazole plantazolicin A and its biosynthetic precursor plantazolicin B. *Angew. Chem., Int. Ed. 54*, 1284−1288.

(11) Wada, H., Williams, H. E., and Moody, C. J. (2015) Total synthesis of the posttranslationally modified polyazole peptide antibiotic plantazolicin A. *Angew. Chem., Int. Ed. 54*, 15147.

(12) Deane, C. D., Melby, J. O., Molohon, K. J., Susarrey, A. R., and Mitchell, D. A. (2013) Engineering unnatural variants of plantazolicin through codon reprogramming. *ACS Chem. Biol. 8*, 1998−2008.

(13) Lee, J., Hao, Y., Blair, P. M., Melby, J. O., Agarwal, V., Burkhart, B. J., Nair, S. K., and Mitchell, D. A. (2013) Structural and functional insight into an unexpectedly selective *N*-methyltransferase involved in plantazolicin biosynthesis. *Proc. Natl. Acad. Sci. U. S. A. 110*, 12954−12959.

(14) Sharma, A., Blair, P. M., and Mitchell, D. A. (2013) Synthesis of plantazolicin analogues enables dissection of ligand binding interactions of a highly selective methyltransferase. *Org. Lett. 15*, 5076−5079.

(15) Hao, Y., Blair, P. M., Sharma, A., Mitchell, D. A., and Nair, S. K. (2015) Insights into methyltransferase specificity and bioactivity of derivatives of the antibiotic plantazolicin. *ACS Chem. Biol. 10*, 1209−1216.

(16) Lee, S. W., Mitchell, D. A., Markley, A. L., Hensler, M. E., Gonzalez, D., Wohlrab, A., Dorrestein, P. C., Nizet, V., and Dixon, J. E.

DOI: 10.1021/acsinfecdis.5b00115
ACS Infect. Dis. 2016, 2, 207−220

(2008) Discovery of a widely distributed toxin biosynthetic gene cluster. *Proc. Natl. Acad. Sci. U. S. A. 105*, 5879−5884.
(17) Rasko, D. A., Altherr, M. R., Han, C. S., and Ravel, J. (2005) Genomics of the *Bacillus cereus* group of organisms. *FEMS Microbiol. Rev. 29*, 303−329.
(18) Kolsto, A. B., Tourasse, N. J., and Okstad, O. A. (2009) What sets *Bacillus anthracis* apart from other *Bacillus* species? *Annu. Rev. Microbiol. 63*, 451−476.
(19) Mesnage, S., Fontaine, T., Mignot, T., Delepierre, M., Mock, M., and Fouet, A. (2000) Bacterial SLH domain proteins are non-covalently anchored to the cell surface via a conserved mechanism involving wall polysaccharide pyruvylation. *EMBO J. 19*, 4473−4484.
(20) Kern, J., Ryan, C., Faull, K., and Schneewind, O. (2010) *Bacillus anthracis* surface-layer proteins assemble by binding to the secondary cell wall polysaccharide in a manner that requires *csaB* and *tagO*. *J. Mol. Biol. 401*, 757−775.
(21) Weidenmaier, C., and Peschel, A. (2008) Teichoic acids and related cell-wall glycopolymers in Gram-positive physiology and host interactions. *Nat. Rev. Microbiol. 6*, 276−287.
(22) Ganguly, J., Low, L. Y., Kamal, N., Saile, E., Forsberg, L. S., Gutierrez-Sanchez, G., Hoffmaster, A. R., Liddington, R., Quinn, C. P., Carlson, R. W., and Kannenberg, E. L. (2013) The secondary cell wall polysaccharide of *Bacillus anthracis* provides the specific binding ligand for the C-terminal cell wall-binding domain of two phage endolysins, PlyL and PlyG. *Glycobiology 23*, 820−832.
(23) Schuch, R., Pelzek, A. J., Raz, A., Euler, C. W., Ryan, P. A., Winer, B. Y., Farnsworth, A., Bhaskaran, S. S., Stebbins, C. E., Xu, Y., Clifford, A., Bearss, D. J., Vankayalapati, H., Goldberg, A. R., and Fischetti, V. A. (2013) Use of a bacteriophage lysin to identify a novel target for antimicrobial development. *PLoS One 8*, e60754.
(24) Ezzell, J. W., Abshire, T. G., Little, S. F., Lidgerding, B. C., and Brown, C. (1990) Identification of *Bacillus anthracis* by using monoclonal antibody to cell wall galactose-*N*-acetylglucosamine polysaccharide. *J. Clin. Microbiol. 28*, 223−231.
(25) Abshire, T. G., Brown, J. E., and Ezzell, J. W. (2005) Production and validation of the use of gamma phage for identification of *Bacillus anthracis*. *J. Clin. Microbiol. 43*, 4780−4788.
(26) Kan, S., Fornelos, N., Schuch, R., and Fischetti, V. A. (2013) Identification of a ligand on the Wip1 bacteriophage highly specific for a receptor on *B. anthracis*. *J. Bacteriol. 195*, 4355.
(27) Hoffmaster, A. R., Hill, K. K., Gee, J. E., Marston, C. K., De, B. K., Popovic, T., Sue, D., Wilkins, P. P., Avashia, S. B., Drumgoole, R., Helma, C. H., Ticknor, L. O., Okinaka, R. T., and Jackson, P. J. (2006) Characterization of *Bacillus cereus* isolates associated with fatal pneumonias: strains are closely related to *Bacillus anthracis* and harbor *B. anthracis* virulence genes. *J. Clin. Microbiol. 44*, 3352−3360.
(28) Schuch, R., and Fischetti, V. A. (2006) Detailed genomic analysis of the Wbeta and gamma phages infecting *Bacillus anthracis*: implications for evolution of environmental fitness and antibiotic resistance. *J. Bacteriol. 188*, 3037−3051.
(29) Marston, C. K., Gee, J. E., Popovic, T., and Hoffmaster, A. R. (2006) Molecular approaches to identify and differentiate *Bacillus anthracis* from phenotypically similar *Bacillus* species isolates. *BMC Microbiol. 6*, 22.
(30) Davison, S., Couture-Tosi, E., Candela, T., Mock, M., and Fouet, A. (2005) Identification of the *Bacillus anthracis* (gamma) phage receptor. *J. Bacteriol. 187*, 6742−6749.
(31) Hoffmaster, A. R., Ravel, J., Rasko, D. A., Chapman, G. D., Chute, M. D., Marston, C. K., De, B. K., Sacchi, C. T., Fitzgerald, C., Mayer, L. W., Maiden, M. C., Priest, F. G., Barker, M., Jiang, L., Cer, R. Z., Rilstone, J., Peterson, S. N., Weyant, R. S., Galloway, D. R., Read, T. D., Popovic, T., and Fraser, C. M. (2004) Identification of anthrax toxin genes in a *Bacillus cereus* associated with an illness resembling inhalation anthrax. *Proc. Natl. Acad. Sci. U. S. A. 101*, 8449−8454.
(32) Burkett-Cadena, M., Kokalis-Burelle, N., Lawrence, K. S., van Santen, E., and Kloepper, J. W. (2008) Suppressiveness of root-knot nematodes mediated by rhizobacteria. *Biol. Control 47*, 55−59.
(33) Liu, Z., Budiharjo, A., Wang, P., Shi, H., Fang, J., Borriss, R., Zhang, K., and Huang, X. (2013) The highly modified microcin peptide plantazolicin is associated with nematicidal activity of *Bacillus amyloliquefaciens* FZB42. *Appl. Microbiol. Biotechnol. 97*, 10081−10090.
(34) Ziegler, S., Pries, V., Hedberg, C., and Waldmann, H. (2013) Target identification for small bioactive molecules: finding the needle in the haystack. *Angew. Chem., Int. Ed. 52*, 2744−2792.
(35) Burdine, L., and Kodadek, T. (2004) Target identification in chemical genetics: the (often) missing link. *Chem. Biol. 11*, 593−597.
(36) Hobbs, J. K., Miller, K., O'Neill, A. J., and Chopra, I. (2008) Consequences of daptomycin-mediated membrane damage in *Staphylococcus aureus*. *J. Antimicrob. Chemother. 62*, 1003−1008.
(37) Sahl, H. G., and Brandis, H. (1982) Mode of action of the staphylococcin-like peptide Pep 5 and culture conditions effecting its activity. *Zentralbl. Bakteriol. Mikrobiol. Hyg. A 252*, 166−175.
(38) Brazas, M. D., and Hancock, R. E. (2005) Using microarray gene signatures to elucidate mechanisms of antibiotic action and resistance. *Drug Discovery Today 10*, 1245−1252.
(39) Shaw, K. J., and Morrow, B. J. (2003) Transcriptional profiling and drug discovery. *Curr. Opin. Pharmacol. 3*, 508−512.
(40) Li, X. Z., and Nikaido, H. (2009) Efflux-mediated drug resistance in bacteria: an update. *Drugs 69*, 1555−1623.
(41) Jordan, S., Hutchings, M. I., and Mascher, T. (2008) Cell envelope stress response in Gram-positive bacteria. *FEMS Microbiol. Rev. 32*, 107−146.
(42) Wecke, T., Zuhlke, D., Mader, U., Jordan, S., Voigt, B., Pelzer, S., Labischinski, H., Homuth, G., Hecker, M., and Mascher, T. (2009) Daptomycin versus friulimicin B: in-depth profiling of *Bacillus subtilis* cell envelope stress responses. *Antimicrob. Agents Chemother. 53*, 1619−1623.
(43) Martin, M., and de Mendoza, D. (2013) Regulation of *Bacillus subtilis* DesK thermosensor by lipids. *Biochem. J. 451*, 269−275.
(44) Novo, D., Perlmutter, N. G., Hunt, R. H., and Shapiro, H. M. (1999) Accurate flow cytometric membrane potential measurement in bacteria using diethyloxacarbocyanine and a ratiometric technique. *Cytometry 35*, 55−63.
(45) Ruhr, E., and Sahl, H. G. (1985) Mode of action of the peptide antibiotic nisin and influence on the membrane potential of whole cells and on cytoplasmic and artificial membrane vesicles. *Antimicrob. Agents Chemother. 27*, 841−845.
(46) Silverman, J. A., Perlmutter, N. G., and Shapiro, H. M. (2003) Correlation of daptomycin bactericidal activity and membrane depolarization in *Staphylococcus aureus*. *Antimicrob. Agents Chemother. 47*, 2538−2544.
(47) Epand, R. M., Walker, C., Epand, R. F., and Magarvey, N. A. (2015) Molecular mechanisms of membrane targeting antibiotics. *Biochim. Biophys. Acta, Biomembr.*, DOI: 10.1016/j.bbamem.2015.10.018.
(48) Berenbaum, M. C. (1989) What is synergy? *Pharmacol. Rev. 41*, 93−141.
(49) Tiyanont, K., Doan, T., Lazarus, M. B., Fang, X., Rudner, D. Z., and Walker, S. (2006) Imaging peptidoglycan biosynthesis in *Bacillus subtilis* with fluorescent antibiotics. *Proc. Natl. Acad. Sci. U. S. A. 103*, 11033−11038.
(50) Bindman, N. A., and van der Donk, W. A. (2013) A general method for fluorescent labeling of the N-termini of lanthipeptides and its application to visualize their cellular localization. *J. Am. Chem. Soc. 135*, 10362−10371.
(51) Huang, B., Wang, W., Bates, M., and Zhuang, X. (2008) Three-dimensional super-resolution imaging by stochastic optical reconstruction microscopy. *Science 319*, 810−813.
(52) Nguyen-Mau, S. M., Oh, S. Y., Kern, V. J., Missiakas, D. M., and Schneewind, O. (2012) Secretion genes as determinants of *Bacillus anthracis* chain length. *J. Bacteriol. 194*, 3841−3850.
(53) Silver, L. L. (2011) Challenges of antibacterial discovery. *Clin. Microbiol. Rev. 24*, 71−109.
(54) Deng, W., Li, C., and Xie, J. (2013) The underling mechanism of bacterial TetR/AcrR family transcriptional repressors. *Cell. Signalling 25*, 1608−1613.

DOI: 10.1021/acsinfecdis.5b00115
ACS Infect. Dis. 2016, 2, 207−220

(55) Poelarends, G. J., Mazurkiewicz, P., and Konings, W. N. (2002) Multidrug transporters and antibiotic resistance in *Lactococcus lactis*. *Biochim. Biophys. Acta, Bioenerg. 1555*, 1−7.
(56) Collins, B., Curtis, N., Cotter, P. D., Hill, C., and Ross, R. P. (2010) The ABC transporter AnrAB contributes to the innate resistance of *Listeria monocytogenes* to nisin, bacitracin, and various beta-lactam antibiotics. *Antimicrob. Agents Chemother. 54*, 4416−4423.
(57) Yang, D. C., Peters, N. T., Parzych, K. R., Uehara, T., Markovski, M., and Bernhardt, T. G. (2011) An ATP-binding cassette transporter-like complex governs cell-wall hydrolysis at the bacterial cytokinetic ring. *Proc. Natl. Acad. Sci. U. S. A. 108*, E1052−E1060.
(58) Garti-Levi, S., Hazan, R., Kain, J., Fujita, M., and Ben-Yehuda, S. (2008) The FtsEX ABC transporter directs cellular differentiation in *Bacillus subtilis*. *Mol. Microbiol. 69*, 1018−1028.
(59) Friedman, L., Alder, J. D., and Silverman, J. A. (2006) Genetic changes that correlate with reduced susceptibility to daptomycin in *Staphylococcus aureus*. *Antimicrob. Agents Chemother. 50*, 2137−2145.
(60) Lee, J. Y., Janes, B. K., Passalacqua, K. D., Pfleger, B. F., Bergman, N. H., Liu, H., Hakansson, K., Somu, R. V., Aldrich, C. C., Cendrowski, S., Hanna, P. C., and Sherman, D. H. (2007) Biosynthetic analysis of the petrobactin siderophore pathway from *Bacillus anthracis*. *J. Bacteriol. 189*, 1698−1710.
(61) Zhang, T., Muraih, J. K., Tishbi, N., Herskowitz, J., Victor, R. L., Silverman, J., Uwumarenogie, S., Taylor, S. D., Palmer, M., and Mintzer, E. (2014) Cardiolipin prevents membrane translocation and permeabilization by daptomycin. *J. Biol. Chem. 289*, 11584−11591.
(62) Palmer, K. L., Daniel, A., Hardy, C., Silverman, J., and Gilmore, M. S. (2011) Genetic basis for daptomycin resistance in Enterococci. *Antimicrob. Agents Chemother. 55*, 3345−3356.
(63) Mileykovskaya, E., and Dowhan, W. (2000) Visualization of phospholipid domains in *Escherichia coli* by using the cardiolipin-specific fluorescent dye 10-*N*-nonyl acridine orange. *J. Bacteriol. 182*, 1172−1175.
(64) Mileykovskaya, E., and Dowhan, W. (2009) Cardiolipin membrane domains in prokaryotes and eukaryotes. *Biochim. Biophys. Acta, Biomembr. 1788*, 2084−2091.
(65) Strahl, H., Burmann, F., and Hamoen, L. W. (2014) The actin homologue MreB organizes the bacterial cell membrane. *Nat. Commun. 5*, 3442.
(66) Romantsov, T., Guan, Z., and Wood, J. M. (2009) Cardiolipin and the osmotic stress responses of bacteria. *Biochim. Biophys. Acta, Biomembr. 1788*, 2092−2100.
(67) Peters, A. C., Thomas, L., and Wimpenny, J. W. (1991) Effects of salt concentration on bacterial growth on plates with gradients of pH and temperature. *FEMS Microbiol. Lett. 77*, 309−314.
(68) Unsay, J. D., Cosentino, K., Subburaj, Y., and Garcia-Saez, A. J. (2013) Cardiolipin effects on membrane structure and dynamics. *Langmuir 29*, 15878−15887.
(69) Aguilar, P. S., Cronan, J. E., Jr., and de Mendoza, D. (1998) A *Bacillus subtilis* gene induced by cold shock encodes a membrane phospholipid desaturase. *J. Bacteriol. 180*, 2194−2200.
(70) Hotta, K., Kim, C. Y., Fox, D. T., and Koppisch, A. T. (2010) Siderophore-mediated iron acquisition in *Bacillus anthracis* and related strains. *Microbiology 156*, 1918−1925.
(71) Steil, L., Hoffmann, T., Budde, I., Volker, U., and Bremer, E. (2003) Genome-wide transcriptional profiling analysis of adaptation of *Bacillus subtilis* to high salinity. *J. Bacteriol. 185*, 6358−6370.
(72) Hoffmann, T., Schutz, A., Brosius, M., Volker, A., Volker, U., and Bremer, E. (2002) High-salinity-induced iron limitation in *Bacillus subtilis*. *J. Bacteriol. 184*, 718−727.
(73) Ohta, A., Obara, T., Asami, Y., and Shibuya, I. (1985) Molecular cloning of the cls gene responsible for cardiolipin synthesis in *Escherichia coli* and phenotypic consequences of its amplification. *J. Bacteriol. 163*, 506−514.
(74) Kellogg, D. S., Jr., Peacock, W. L., Jr., Deacon, W. E., Brown, L., and Pirkle, D. I. (1963) *Neisseria gonorrhoeae*. I. Virulence genetically linked to clonal variation. *J. Bacteriol. 85*, 1274−1279.
(75) (2006) Clinical and Laboratory Standards Institute. *Methods for Dilution Antimicrobial Susceptibility Tests for Bacteria that Grow Aerobically*, 7th ed. (Approved Standard), CLSI, Wayne, PA, USA.
(76) McClure, R., Balasubramanian, D., Sun, Y., Bobrovskyy, M., Sumby, P., Genco, C. A., Vanderpool, C. K., and Tjaden, B. (2013) Computational analysis of bacterial RNA-Seq data. *Nucleic Acids Res. 41*, e140.
(77) Rust, M. J., Bates, M., and Zhuang, X. (2006) Sub-diffraction-limit imaging by stochastic optical reconstruction microscopy (STORM). *Nat. Methods 3*, 793−795.
(78) Fei, J., Singh, D., Zhang, Q., Park, S., Balasubramanian, D., Golding, I., Vanderpool, C. K., and Ha, T. (2015) RNA biochemistry. Determination of in vivo target search kinetics of regulatory noncoding RNA. *Science 347*, 1371−1374.
(79) Bates, M., Huang, B., Dempsey, G. T., and Zhuang, X. (2007) Multicolor super-resolution imaging with photo-switchable fluorescent probes. *Science 317*, 1749−1753.

DOI: 10.1021/acsinfecdis.5b00115
ACS Infect. Dis. 2016, 2, 207−220